THE INTERNATIONAL ASTROPARTICLE PHYSICS LANDSCAPE

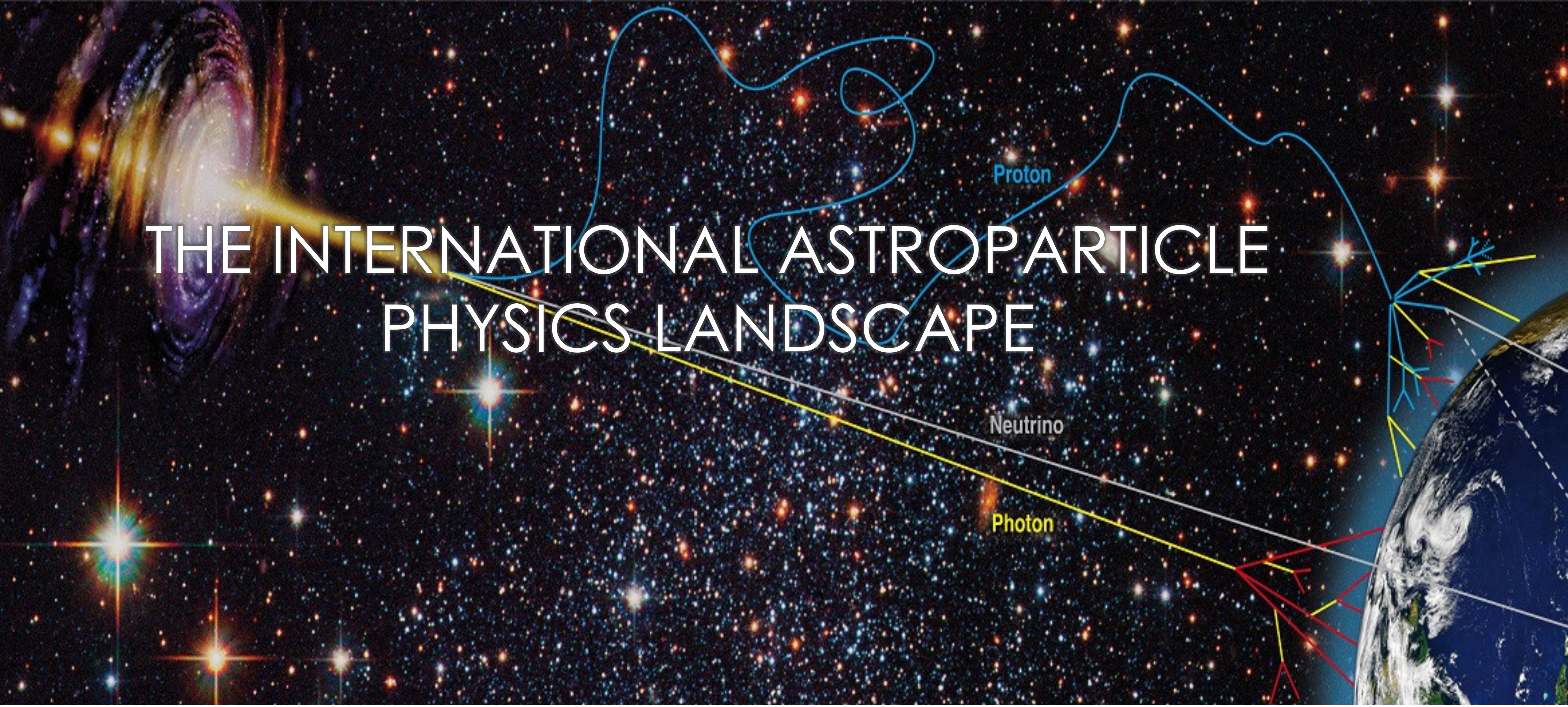

19th February 2021

MOHAMED RAMEEZ

INTERNATIONAL WORKSHOP ON OUTLOOK FOR INO, IICHEP AND BEYOND

Courtesy HAP

Some examples and success stories from exploring synergies

Mainly focusing on IceCube

The IceCube Neutrino Observatory

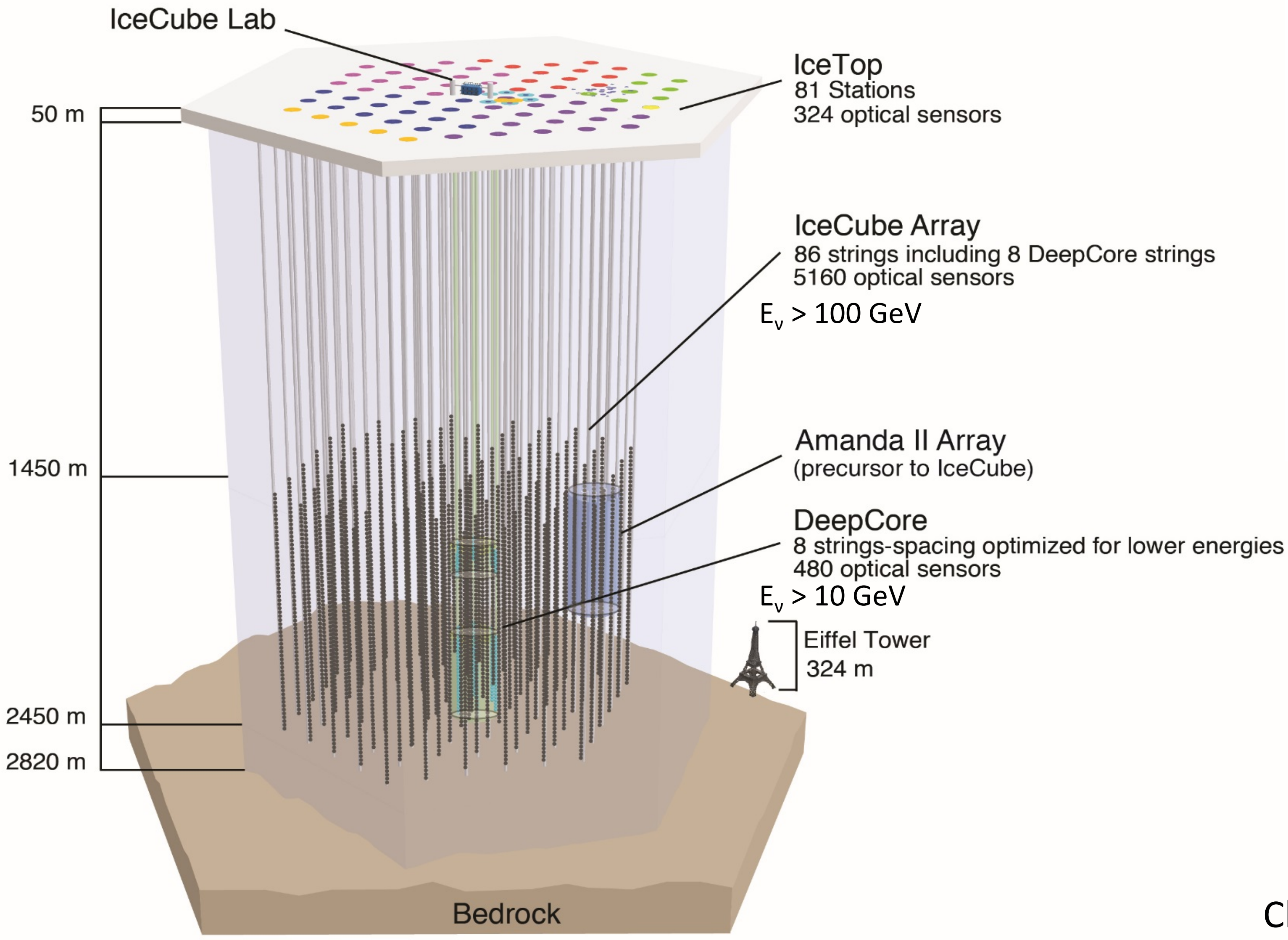

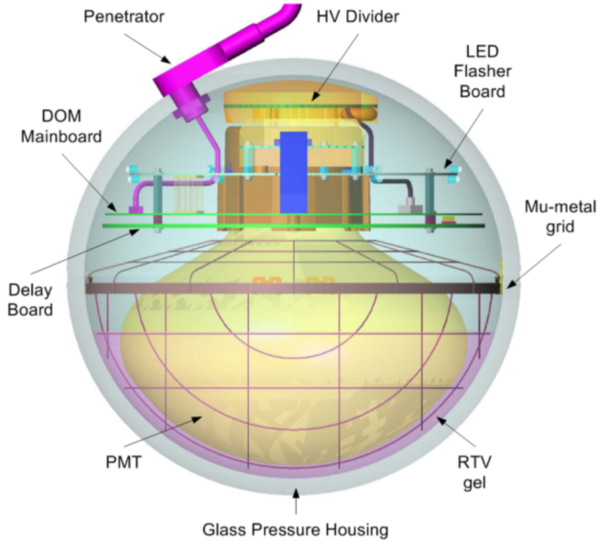

~41^{o} in ice

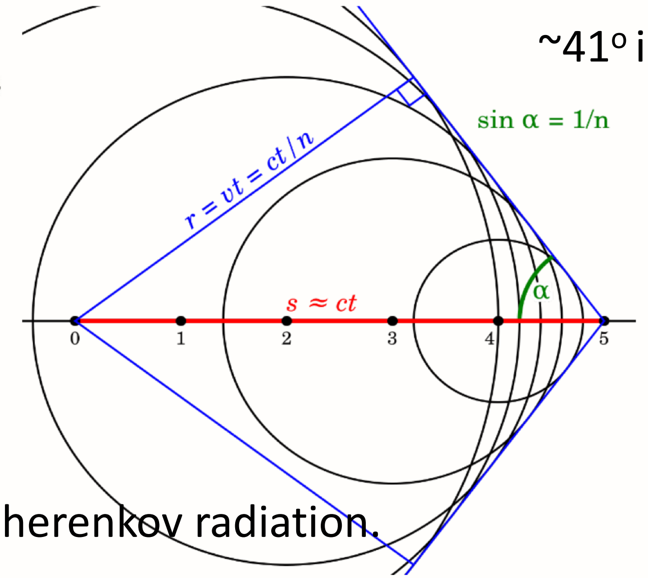

Cherenkov radiation.

In-ice Signatures

Muon tracks→ ν_μ CC

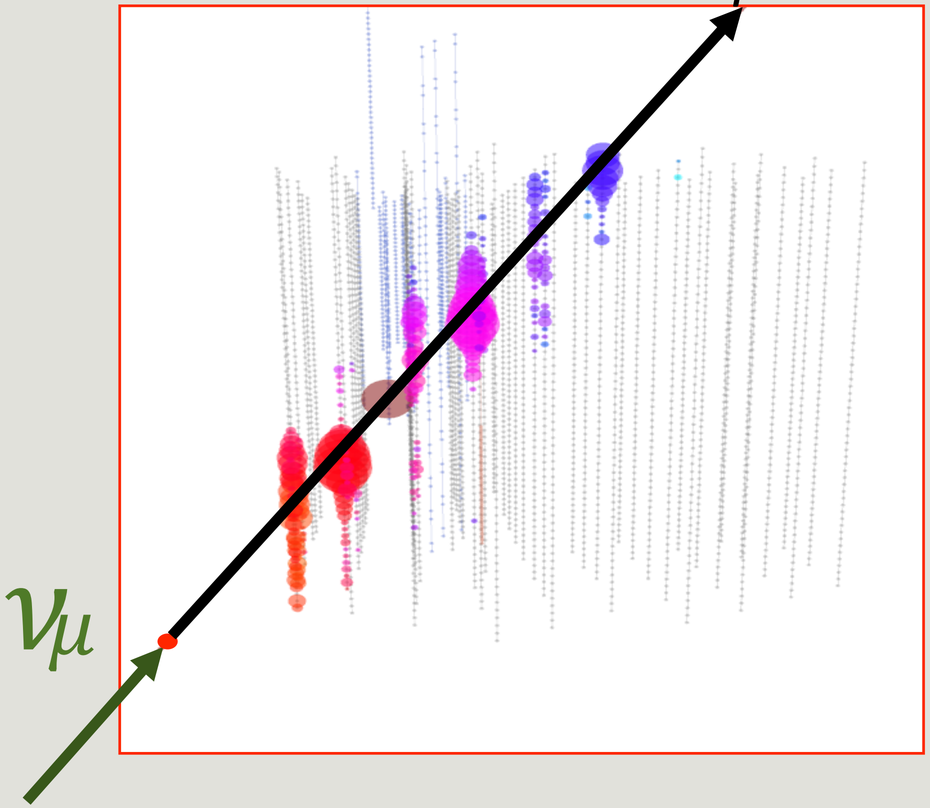

Good angular resolution: **Neutrino Astronomy**

- **(~0.6° at 10 TeV)**
- Vertex can be outside the detector: **Increased effective volume!**

cascades → all flavors

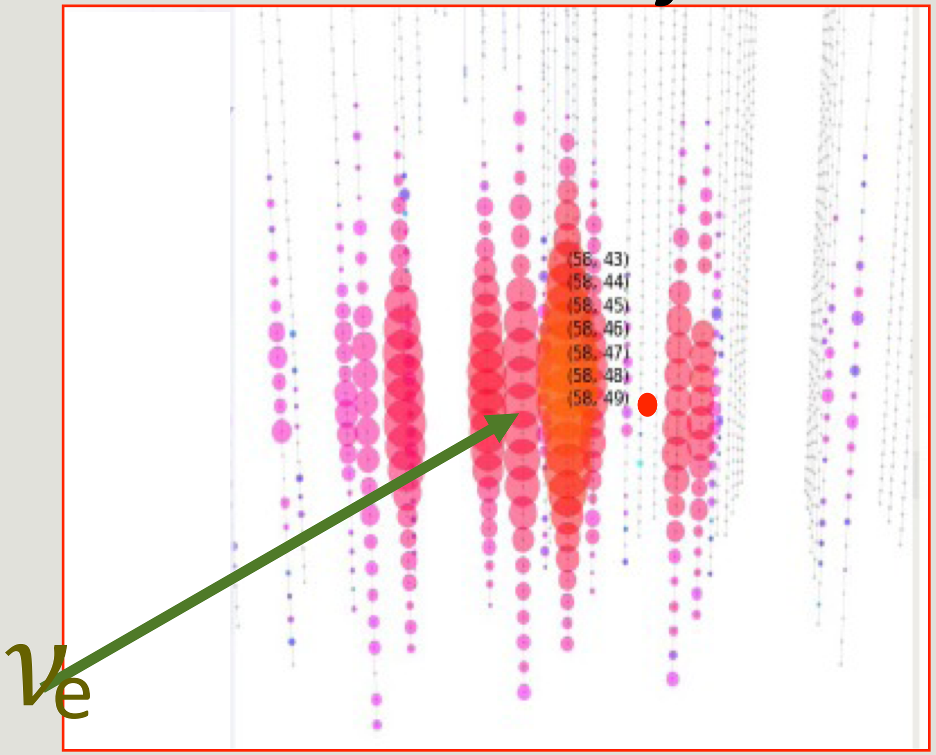

- ν_e, ν_τ and all-flavor neutral current
- Fully active calorimeter: **High energy resolution**
- Angular reconstruction above ~50 TeV

In both cases, ν and $\bar{\nu}$ are indistinguishable

The IceCube astrophysical flux

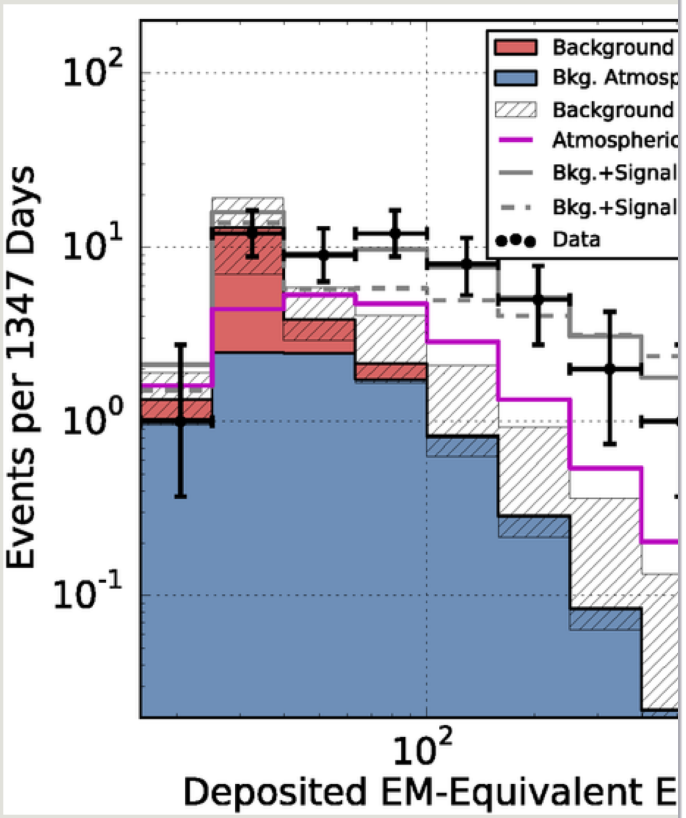

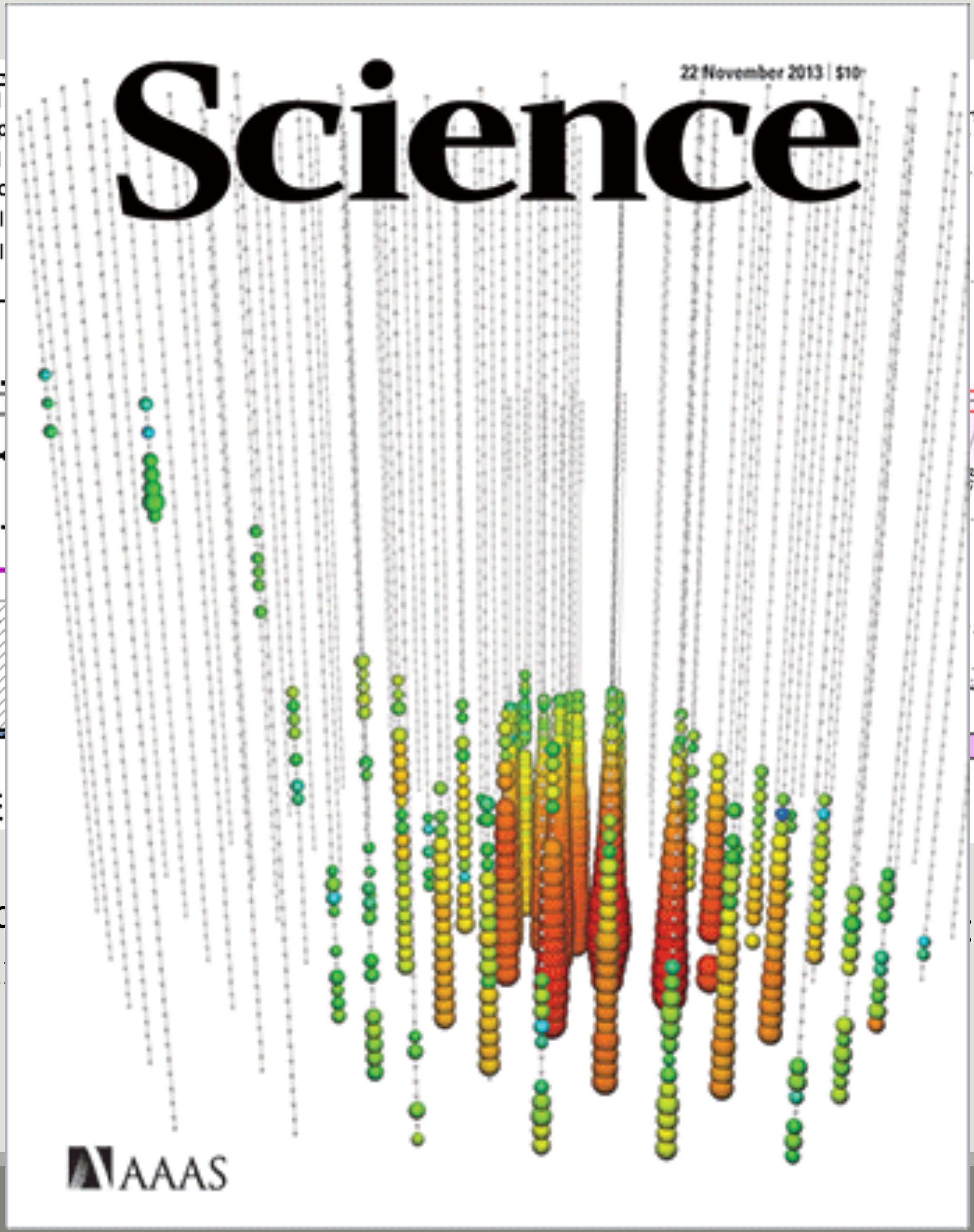

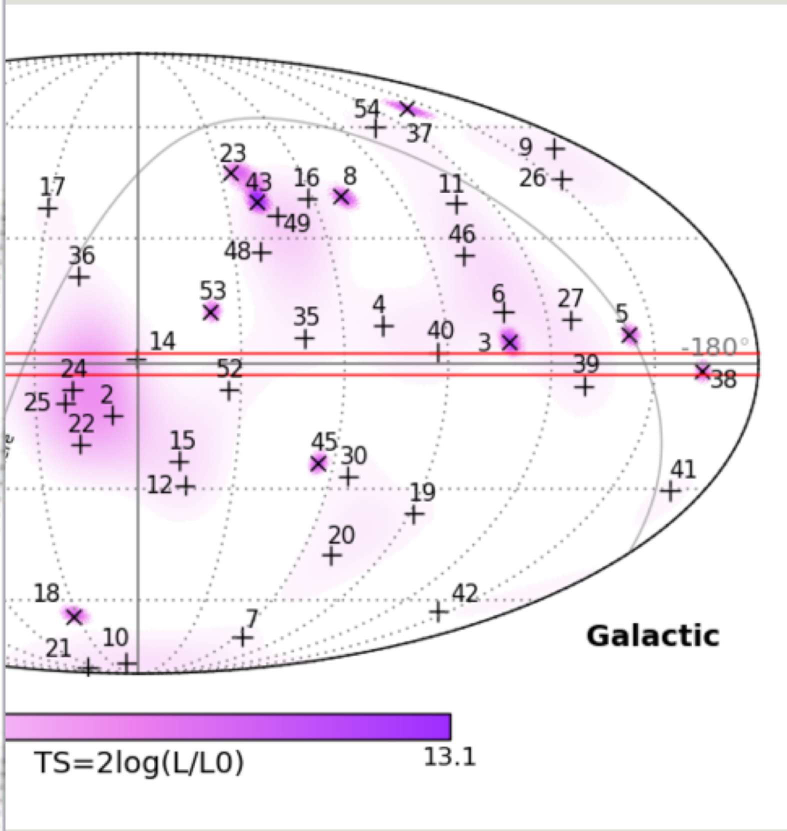

54 events seen on an expected bac

$9.0^{+8.0}_{-2.2}$ ν. Atmospheric only origi

tistically significant clustering

The IceCube astrophysical flux

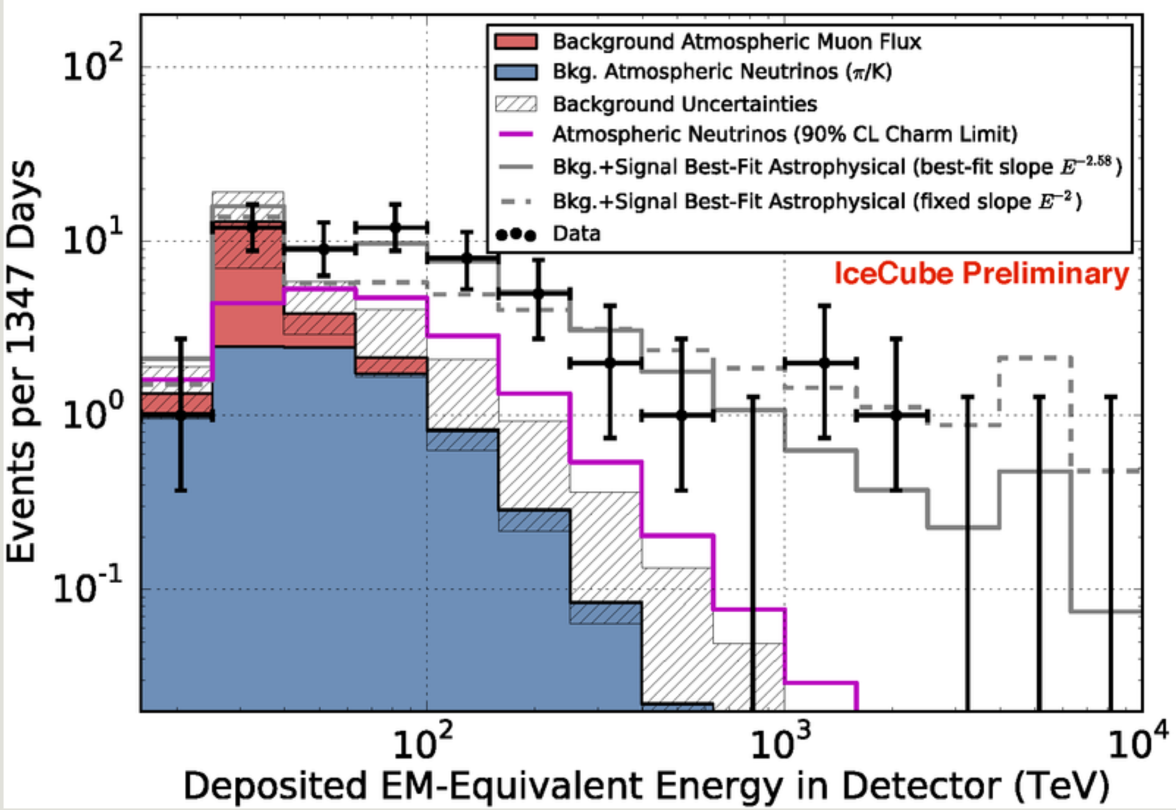

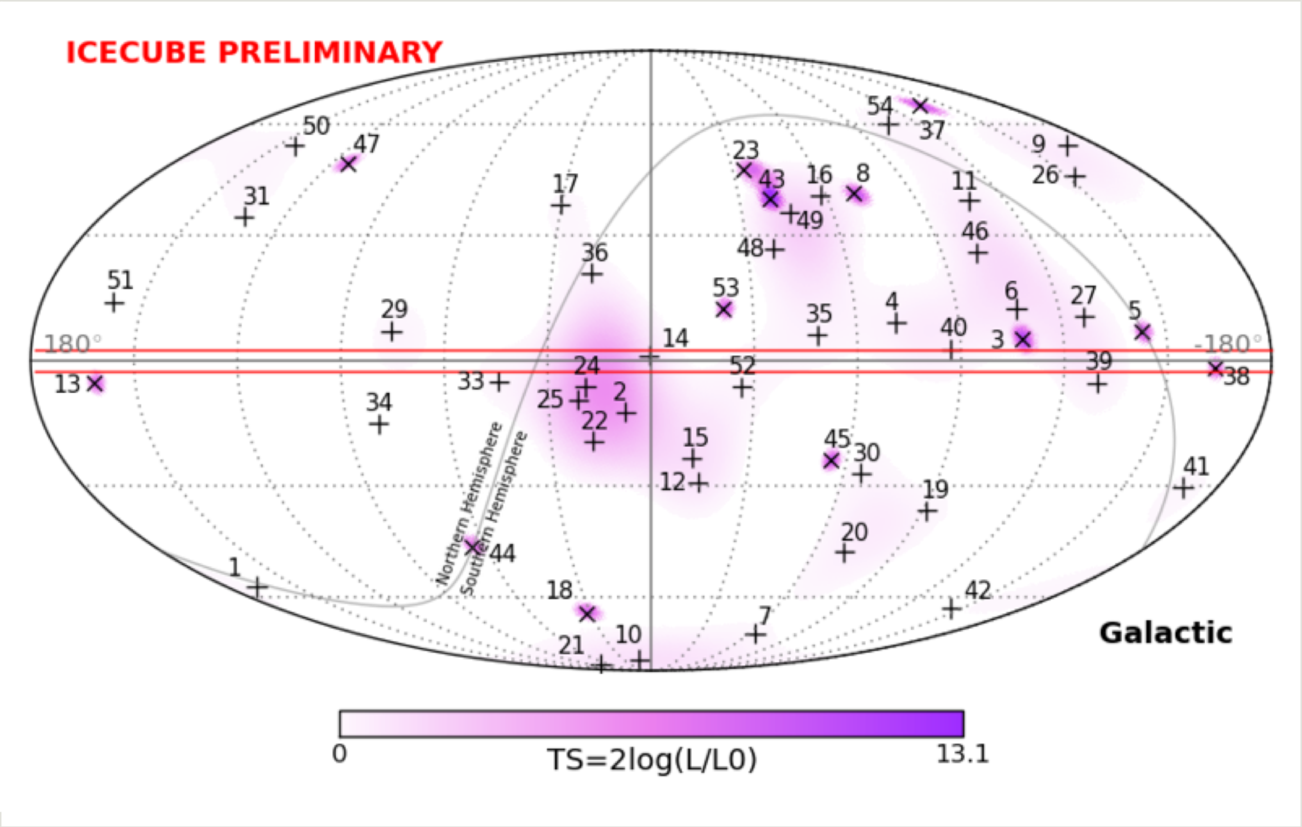

54 events seen on an expected background of $12.6 \pm 5.1\ \mu$ and $9.0^{+8.0}_{-2.2}\ \nu$. Atmospheric only origin rejected at $> 6\sigma$

No statistically significant clustering

Realtime Alerts from IceCube

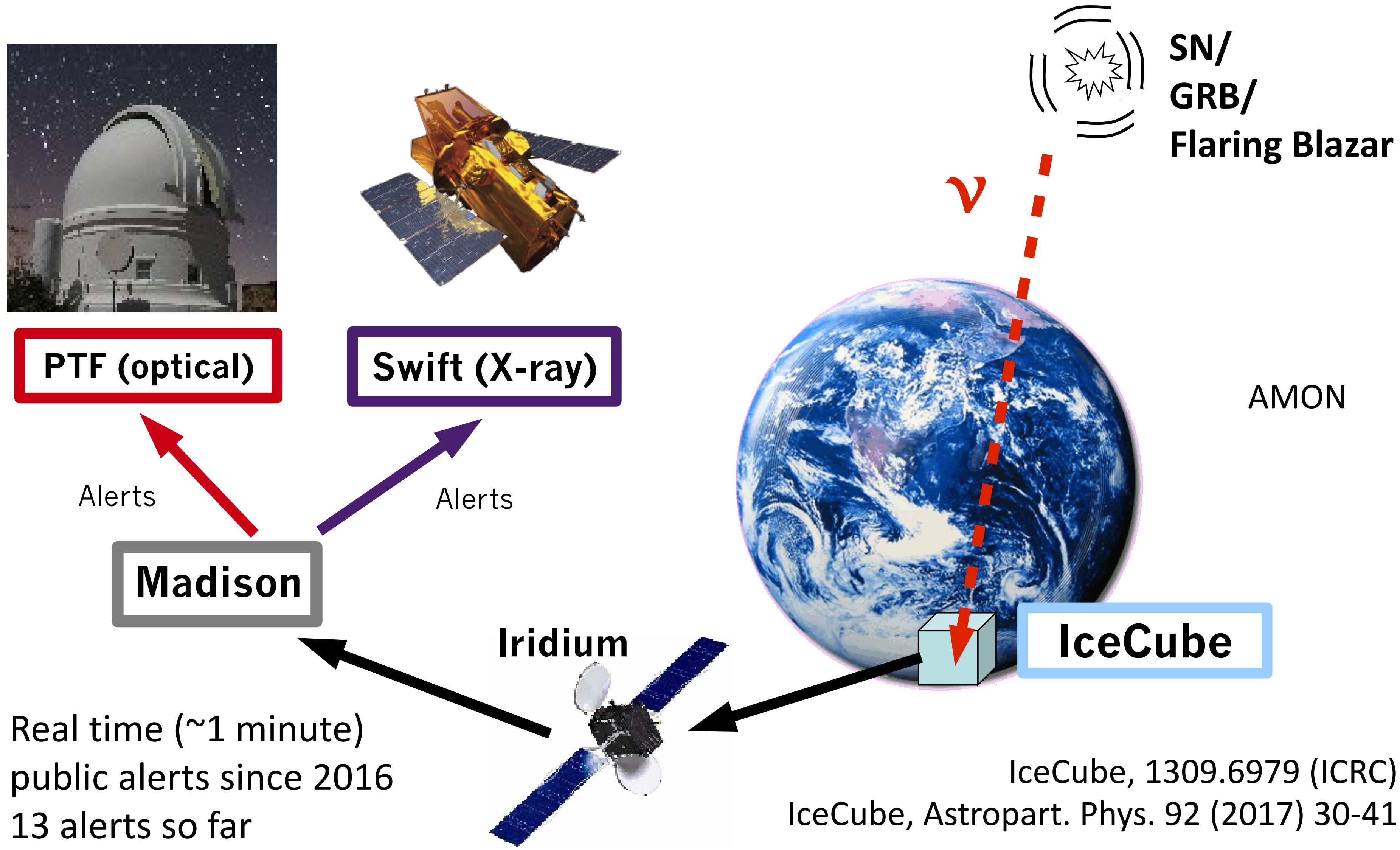

Real time (~1 minute)
public alerts since 2016
13 alerts so far

IceCube, 1309.6979 (ICRC)
IceCube, Astropart. Phys. 92 (2017) 30-41

IceCube-170922: first significant neutrino - gamma ray coincidence

- An event selected with extremely high energy (EHE) event selection (simple requirement of large light deposit)
- Track with ~1°angular resolution, declination = +5.7°
- Coincident with known, flaring Fermi blazar (TXS 0506+056 at z = 0.3)
- No previously known very-high-energy gamma-ray source
- Not detected by H.E.S.S. or VERITAS follow-up
- *In 12-hour follow-up observation, MAGIC detected 5 σ source above 100 GeV*

First-time detection of VHE gamma rays by MAGIC from a direction consistent with the recent EHE neutrino event IceCube-170922A

ATel #10817; ***Razmik Mirzoyan for the MAGIC Collaboration***
on ***4 Oct 2017; 17:17 UT***
Credential Certification: Razmik Mirzoyan (Razmik.Mirzoyan@mpp.mpg.de)

- 21 Astronomers Telegrams
- Also, excess in archival data

Correlations with UHECR arrival directions?

JCAP01(2016)037

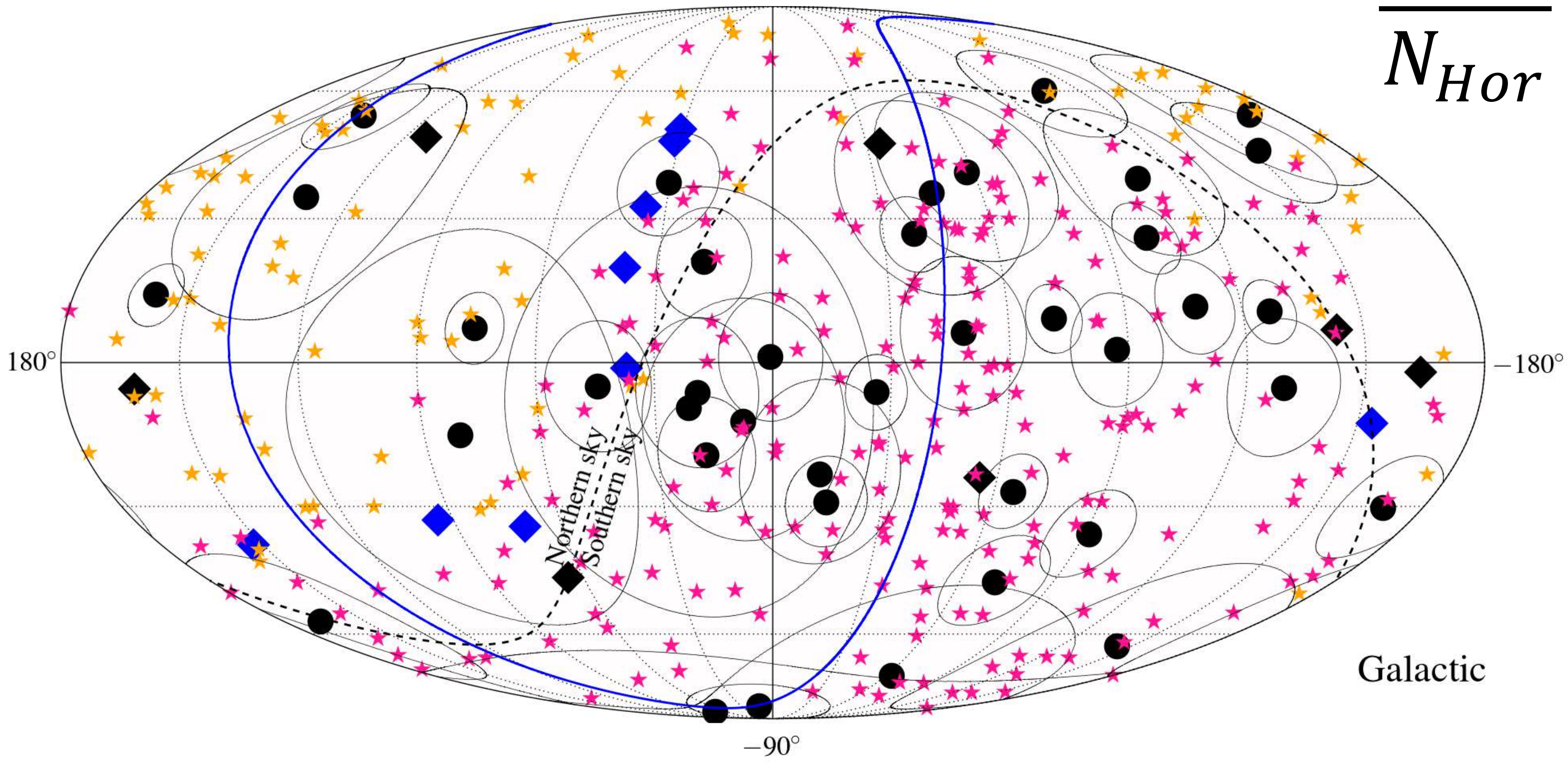

$$\frac{N_{GZK}}{N_{Hor}} < 5\%$$

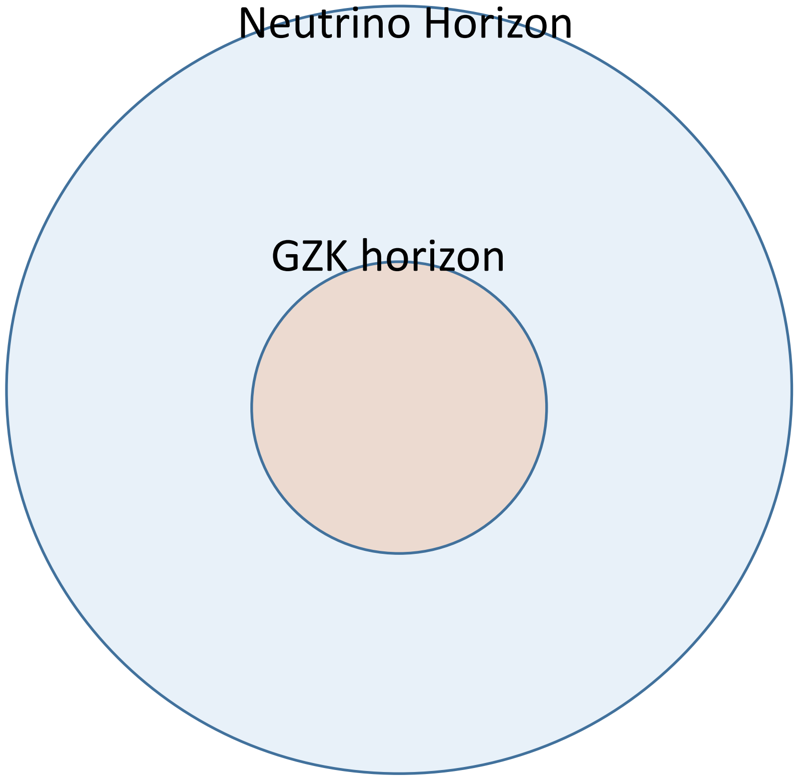

No statistically significant correlation.

DM Capture and Annihilation in the Sun

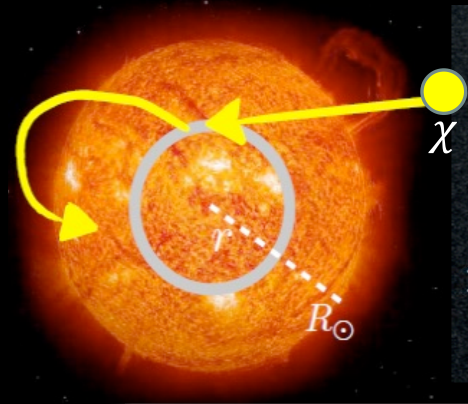

$$\Gamma_{\rm capt} = \frac{\rho_{\rm DM}}{M_{\rm DM}} \sum_i \sigma_i \int_0^{R_\odot} dr\ 4\pi r^2\, n_i(r) \int_0^{\infty} dv\ 4\pi v^2 f_\odot(v)\, \frac{v^2 + v_{\odot \rm esc}^2}{v}\, \wp_i(v, v_{\odot \rm esc})$$

DM number density

Scattering Cross Section
$\sigma_{SD} \propto J(J+1)$
$\sigma_{SI} \propto A^2$

Number density of element i -> Solar Model

velocity distribution (in solar frame, without Sun's gravity)

effect of solar gravity

Spin Dependent scattering

- Only the hydrogen in the Sun contributes significantly.
- Lower event rates in direct detection experiments
- More interesting for IceCube

Spin Independent scattering

- Heavier nuclei contribute more due to $\propto A^2$ enhancement.
- Better sensitivity using direct detection experiments such as LUX, XENON etc

Capture

Equilibrium → $\Gamma_A^{equi} = \frac{1}{2} C_c$

Annihilation

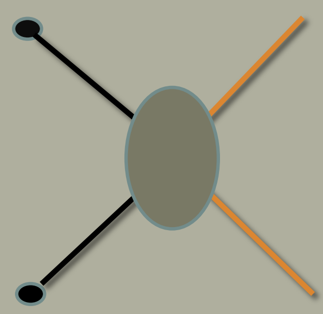

b, W^+, τ^+...

Primary annihilation channels

$\bar{b}, W^-, \tau^-$...

Decay

Dense Medium Interactions
Matter Oscillations

....ν

....$\bar{\nu}$

propagation

Vacuum oscillations

At Earth :
Enhanced neutrino flux from the direction of the Sun!

All calculations performed with DarkSusy/WimpSim

Results (contd)

Assumptions:

- Capture – Annihilation equilibrium
- Standard Maxwellian Halo
- No dark disk
- $\rho_{DM} = 0.3\ GeV\ /cm^3$
- Standard Solar Model
- $v_{sun} = 220\ km/s$

-> Set limit on WIMP-proton scattering cross section

- The best limit is for Spin Dependent $\vec{S}_\chi . \vec{S}_N$ in the language of NR EFTs

(R. Catena et al, JCAP 1504 (2015) 04, 042)

The most stringent limits on SD WIMP-proton cross section above 80 GeV WIMP mass

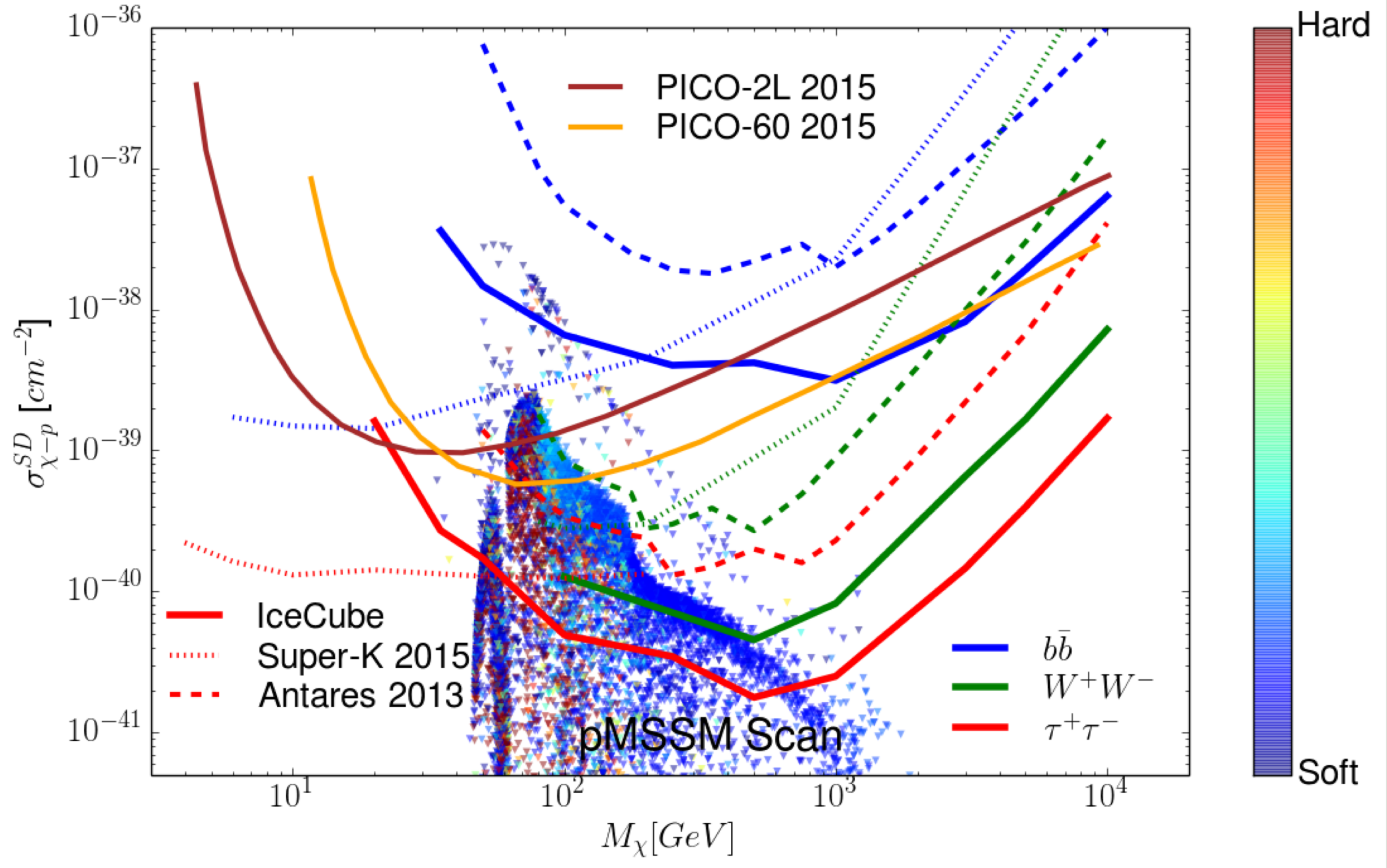

Most stringent bounds

The Standard Maxwellian Halo Velocity distribution function

K, Choi **et al. JCAP05 (2014) 049**

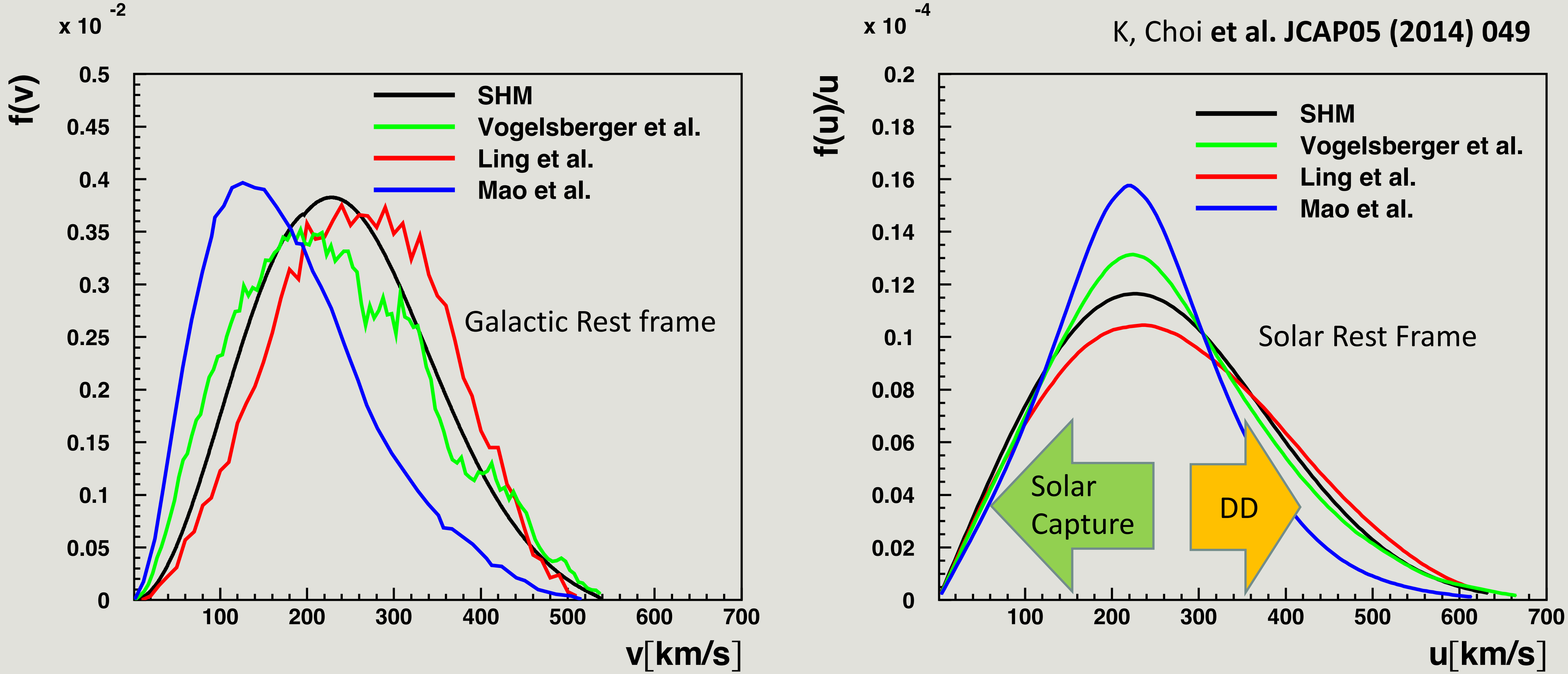

Slower DM particles are more likely to get captured in the Sun
Faster DM particles are more likely to recoil off nuclei in PICO
Deviations from SMH will affect the constraints from the different searches differently

All’s not well with the SMH

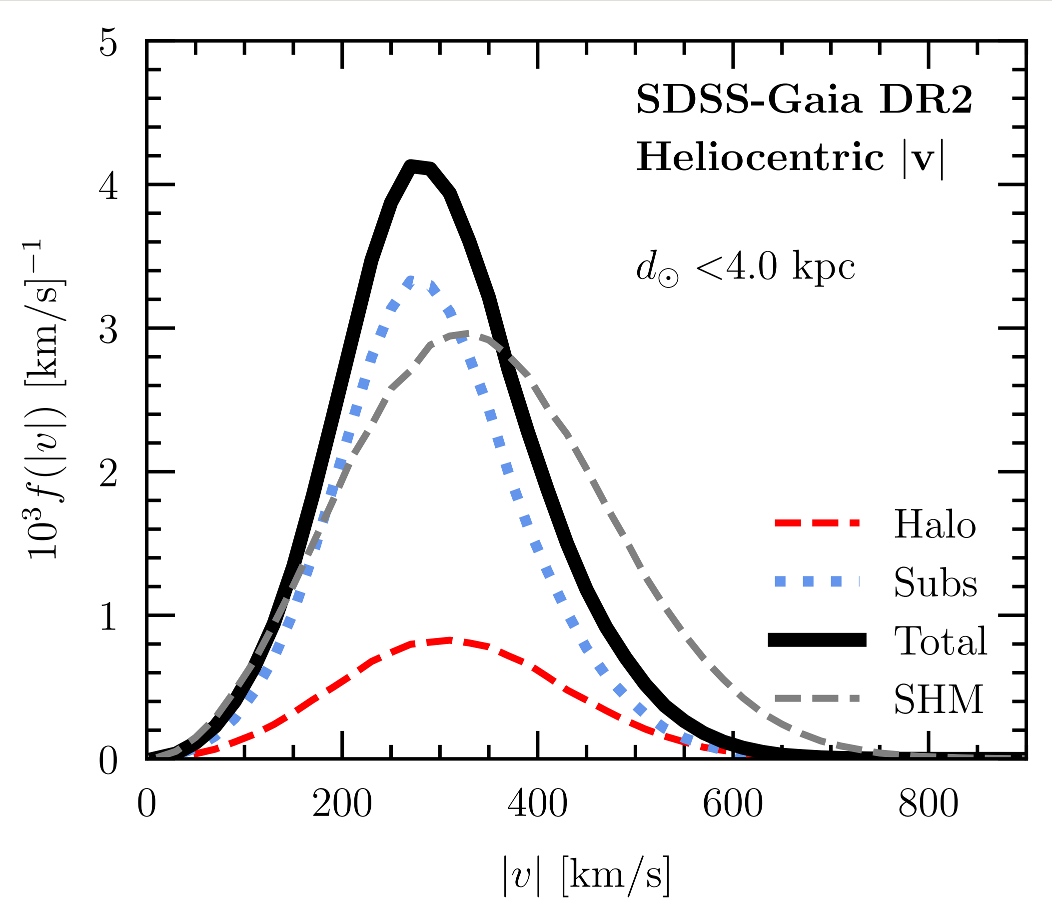

Necib, Lisanti and Belokurov 1807.02519
|Z coord| < 2.5 kpc
4 kpc sphere around the Sun

“the debris from the youngest mergers may be in position and velocity substructure. Referred to as tidal streams, these cold phase-space features tend to trace fragments of a progenitor’s orbit (Zemp et al. 2009; Vo- gelsberger et al. 2009; Diemand et al. 2008; Kuhlen et al. 2010; Maciejewski et al. 2011; Vogelsberger & White 2011; Elahi et al. 2011). ”

Conservative bounds completely independent of the VDF

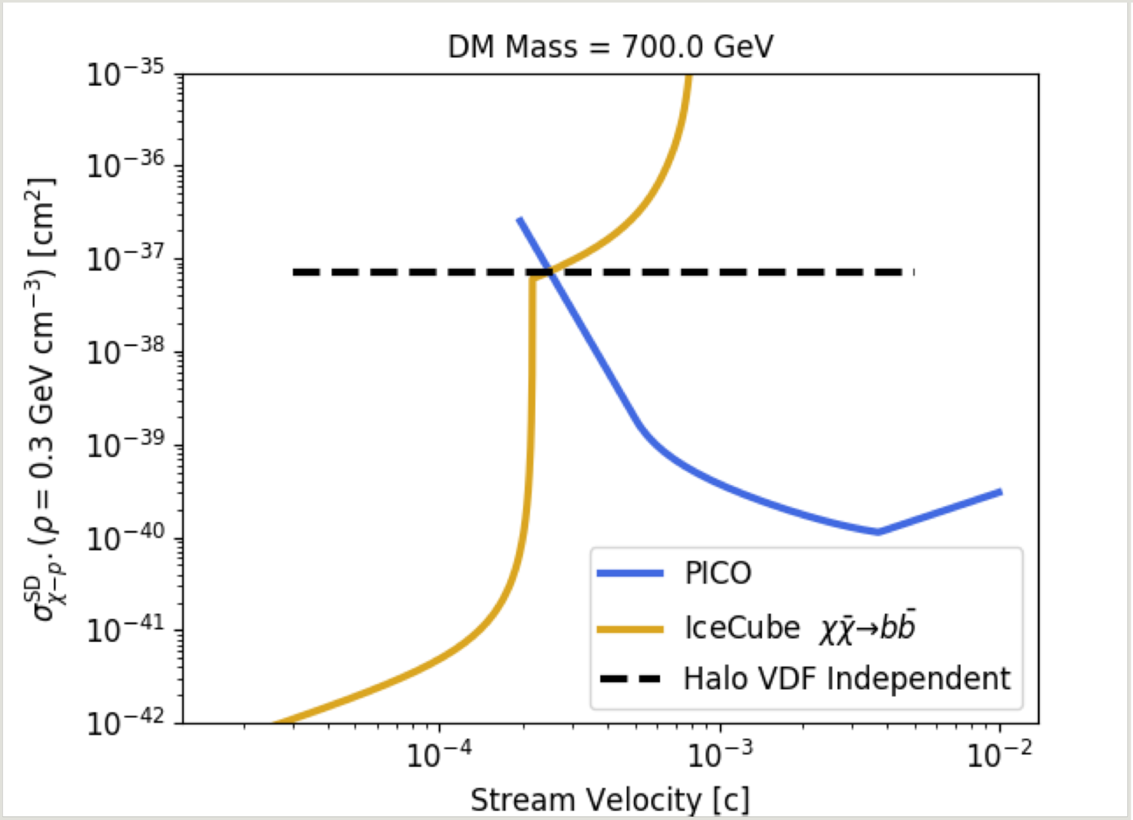

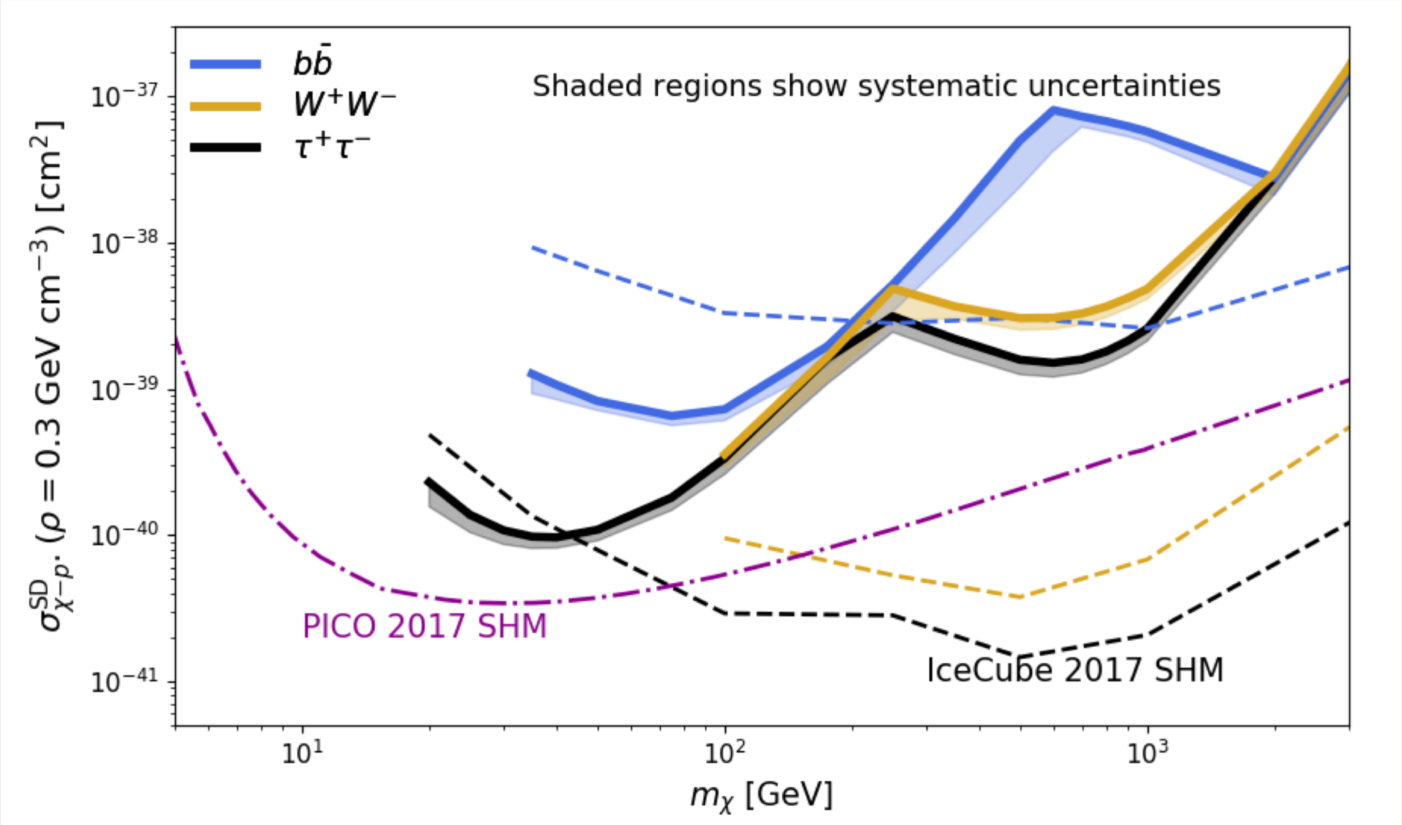

IceCube + PICO synergy, method of Ferrer, Ibarra & White

ν_μ disappearance

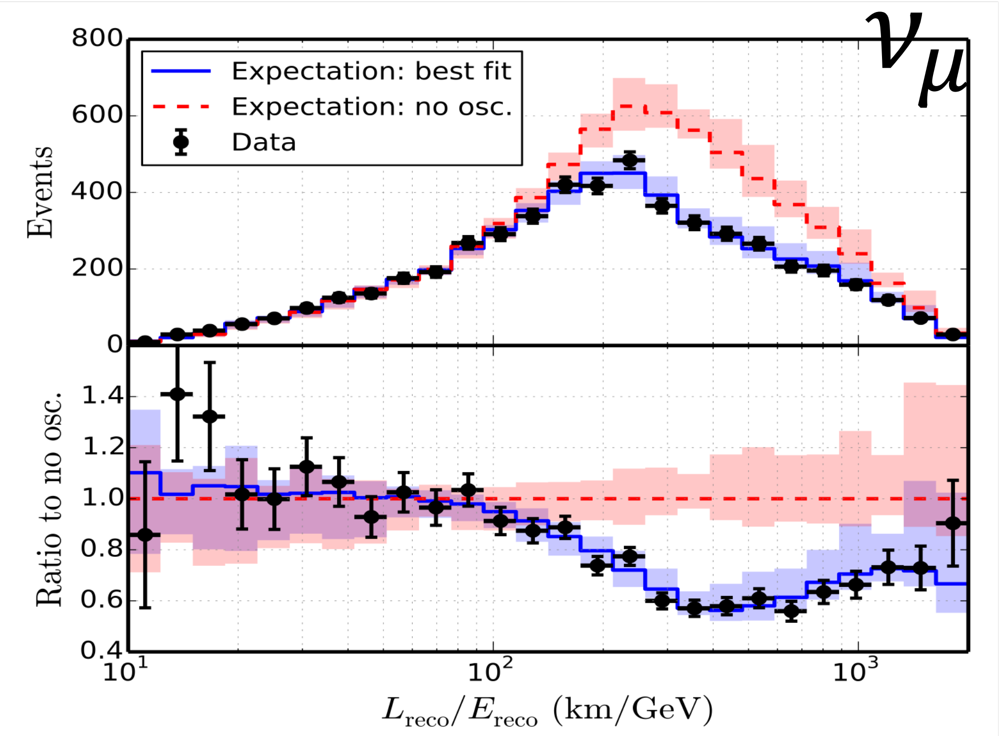

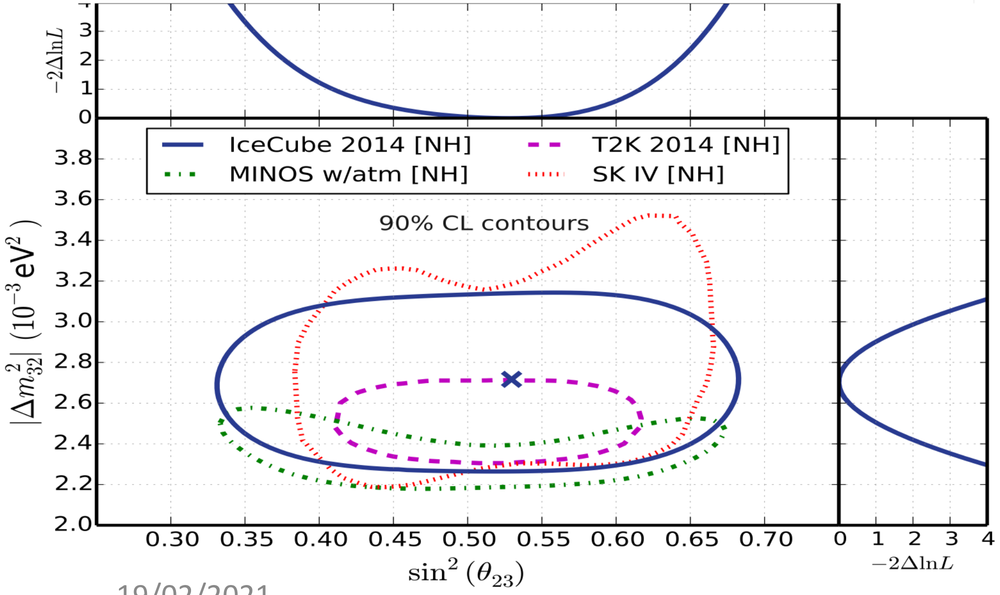

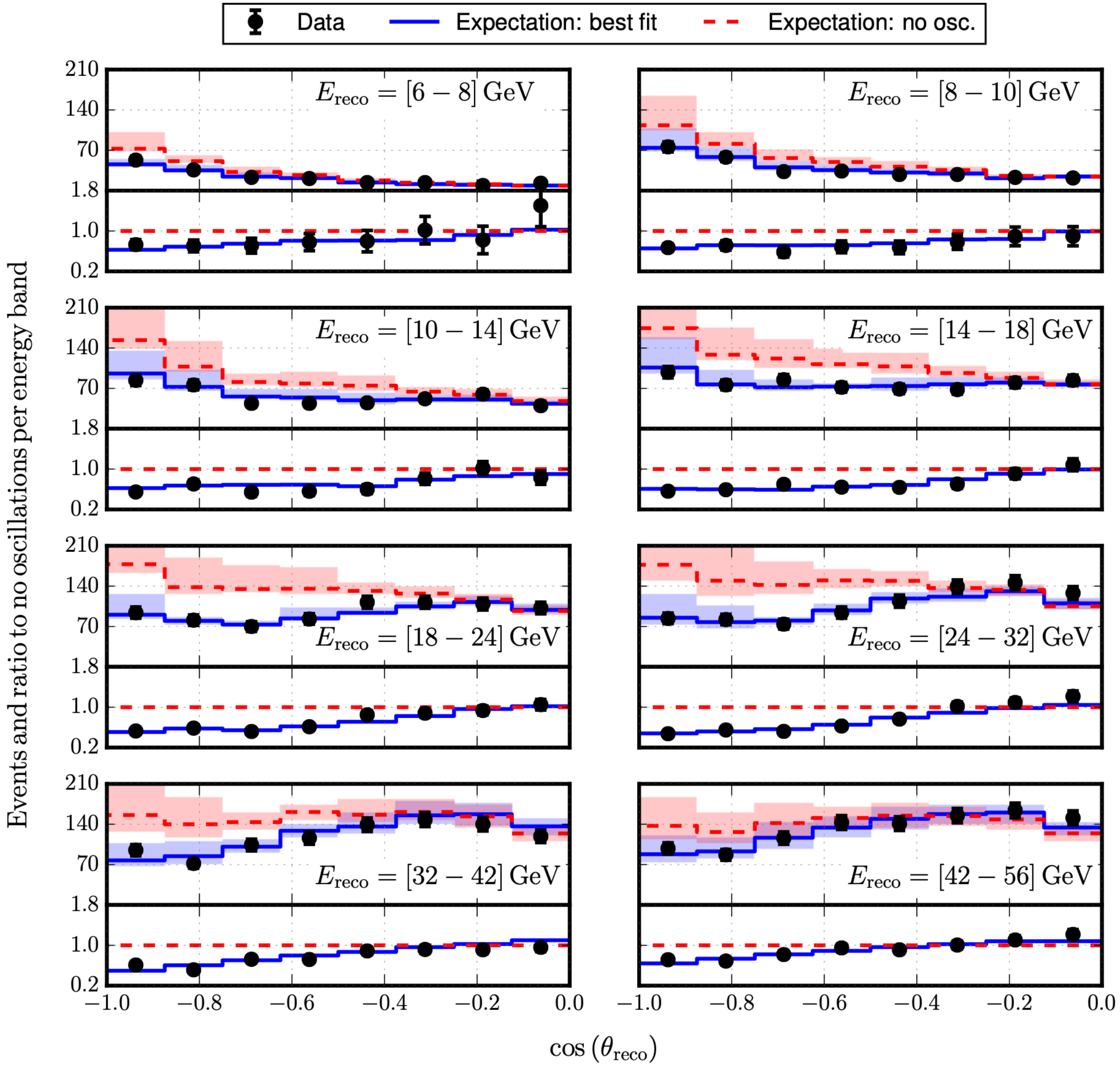

Neutrino Mass Ordering with PINGU/DeepCore

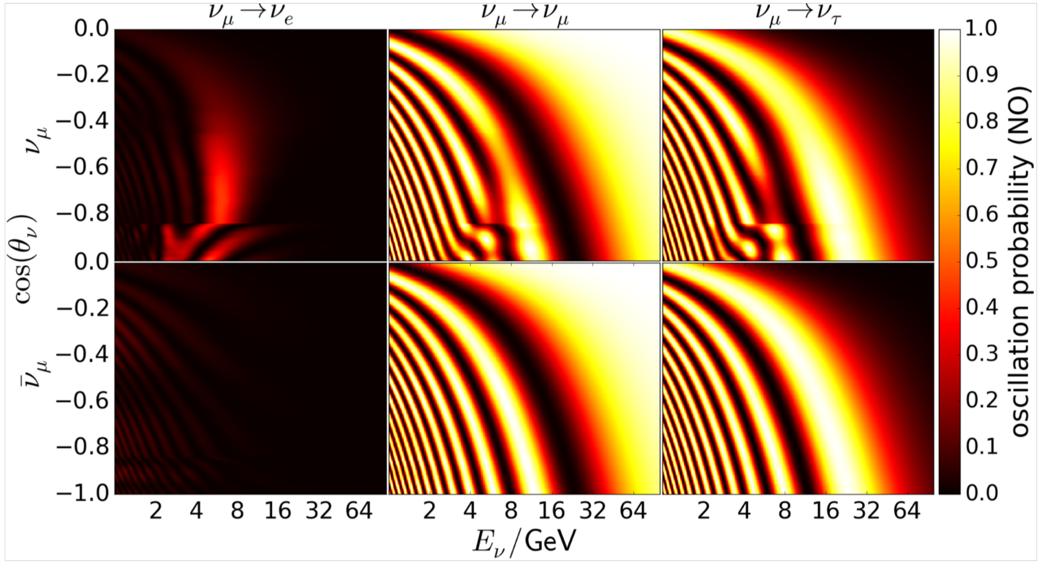

(a) Normal Ordering

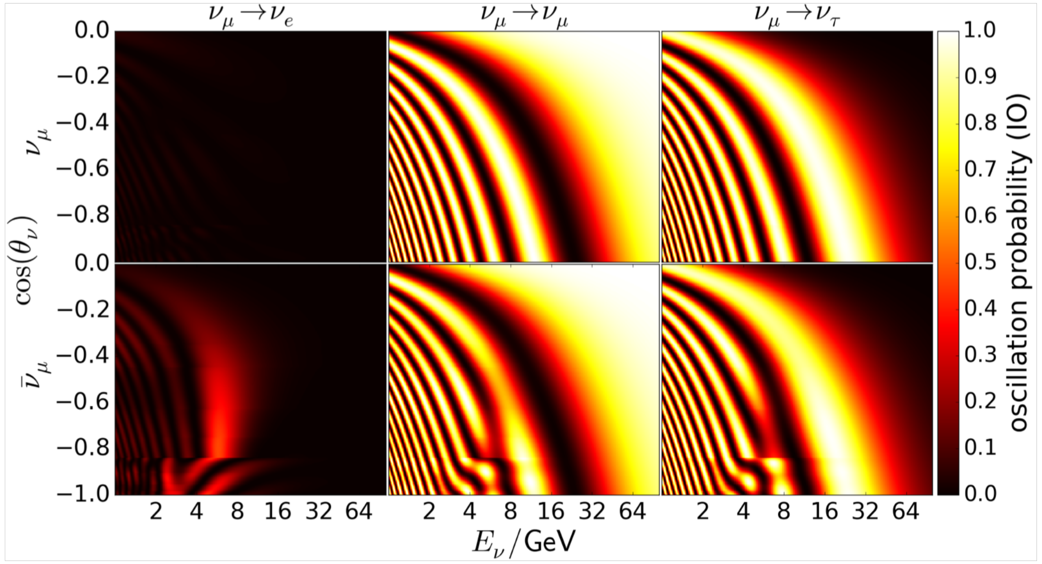

(b) Inverted Ordering

Table 2 Systematics treated as nuisance parameters in the likelihood analysis, including normalization (N), detector response (D), oscillation (O), flux (F), and neutrino-nucleon interaction (I) uncertainties. These parameters are discussed in more detail in [48]. The table gives the baseline value and, if the parameter is used with a prior in the likelihood, the standard deviation of the Gaussian prior, as well as the experimental best-fit values for both analyses and ordering hypotheses.

Label	Type	Description of Parameter	Baseline±Prior	Analysis $\mathcal{A}$		Analysis $\mathcal{B}$	
				NO	IO	NO	IO
N_ν	N, F	normalization of total neutrino template	1[ae]	0.83	0.84	0.98	0.99
N_{ν_e}	N, F	normalization of ν_e flux before oscillations	1 ± 0.05[ad]	1.00	1.00	1.37	1.38
N_{NC}	N, I	normalization of NC events	1 ± 0.2[a]	0.74	0.75	0.99	0.99
N_μ	N, F	normalization of atmos. muon events	1[ae]	1.35	1.34	0.2%[c]	0.2%[c]
ϵ_{opt}	D	overall optical efficiency [13]	1 ± 0.1[ad]	1.00	1.00	0.92	0.92
$\epsilon_{\mathrm{lateral}}$	D	lateral dependence of optical efficiency [13]	0 ± 1[b]	0.68	0.68	-0.46	-0.46
$\epsilon_{\mathrm{head-on}}$	D	head-on optical efficiency [13]	0[be]	-1.01	-1.01	-2.00	-1.92
$\Delta m^2_{31}/(10^{-3}\,\mathrm{eV}^2)$	O	atmospheric mass-splitting	2.5(NO)/−2.43(IO)[e]	2.626	-2.511	2.462	-2.348
$\sin^2(\theta_{23})$	O	atmospheric neutrino mixing angle	0.455[e]	0.476	0.485	0.558	0.539
γ_ν	F	neutrino spectral index unc. [38]	0.0 ± 0.1[d]	0.073	0.071	-0.025	-0.027
γ_μ	F	atmospheric muon spectrum unc. [50, 57]	0.0 ± 1.0[b]	0.04	0.04	–	–
$\sigma_\nu^{\mathrm{zenith}}$	F	zenith-dependent unc. in $\nu/\bar{\nu}$ flux [58]	0.0 ± 1.0[bd]	-0.12	-0.11	-0.86	-0.89
$\Delta(\nu/\bar{\nu})$	F	energy-dependent unc. in $\nu/\bar{\nu}$ ratio [58]	0.0 ± 1.0[b]	-1.03	-1.02	0.05	0.07
M_A^{res}/GeV	I	axial mass unc. of resonant events [39]	1.12 ± 0.22	1.091	1.095	1.003	0.999
M_A^{qe}/GeV	I	axial mass unc. of quasi-elastic events [39]	0.99 ± 0.25	0.862	0.867	0.881	0.888

[a] relative to the nominal value of this parameter
[b] parametrized with respect to the value and the uncertainty obtained from the provided reference
[c] given as fraction of the total sample, since no Monte Carlo prediction exists to compare to
[d] no prior used for likelihood in Analysis $\mathcal{B}$
[e] parameter allowed to vary freely (no prior) in both analyses

PINGU/Upgrade/JUNO Synergy

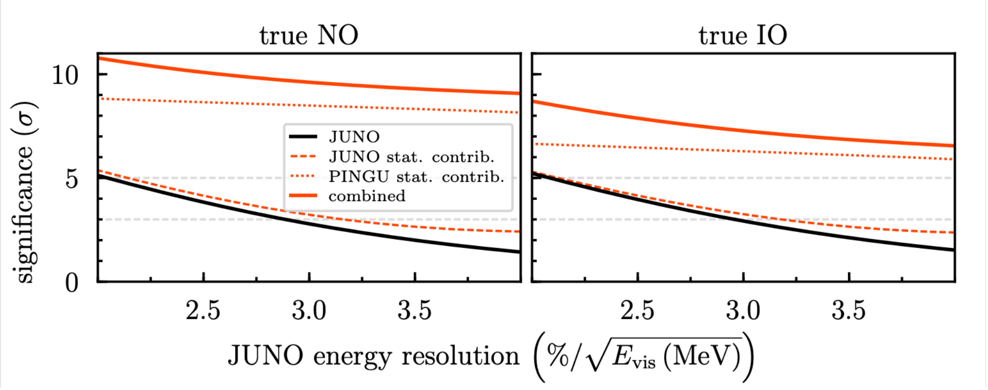

Figure 7. NMO sensitivities (combined, statistical contributions of JUNO and PINGU, JUNO stand-alone) as a function of JUNO's true energy resolution (for true NO on the left, true IO on the right) after 6 years of operation of both experiments.

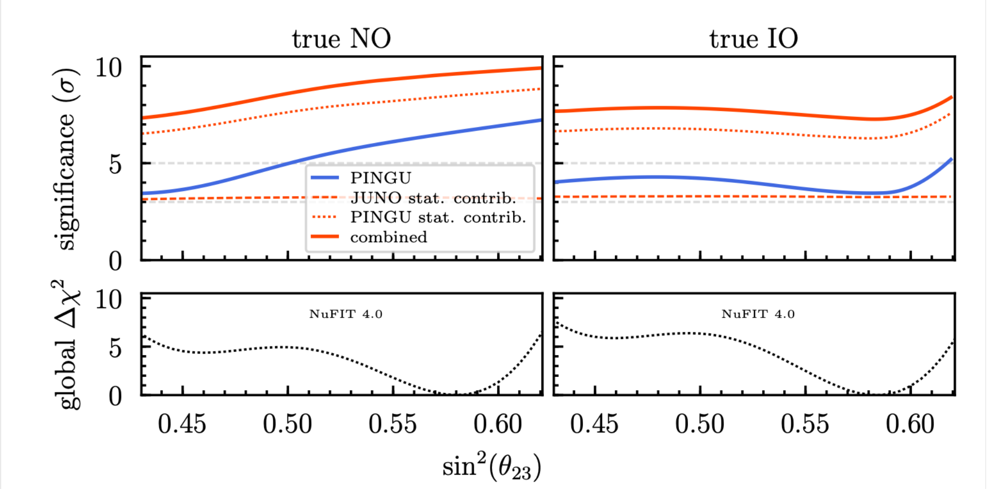

Figure 8. NMO sensitivities (combined, statistical contributions of JUNO and PINGU, PINGU stand-alone) as a function of the true value of $\sin^2(\theta_{23})$ (for true NO on the left, true IO on the right) after 6 years of operation of both experiments. The lower panels show the global $\Delta\chi^2$ constraint on $\sin^2(\theta_{23})$ (relative to the χ^2 minimum within each ordering) from [7, 8].

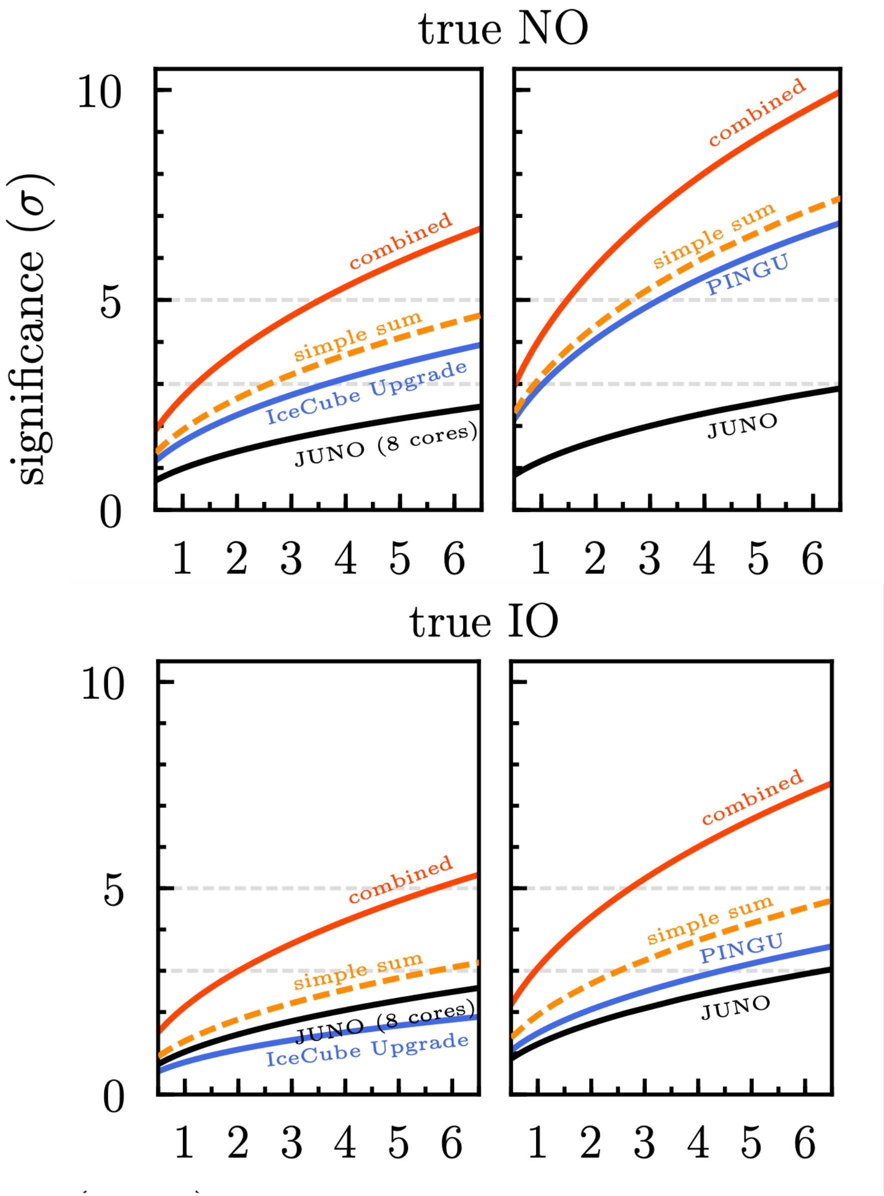

Conclusions

- Synergies between multiple experiments in the last decade have had a multiplier effect.

- ICAL's strength in charge separation must be exploited to augment other experiments.